



A proof of principle experiment for microbeam radiation therapy at the Munich compact light source

Annique C. Dombrowsky^{1,2} · Karin Burger^{2,3,4} · Ann-Kristin Porth² · Marlon Stein^{1,2} · Martin Dierolf^{3,4} · Benedikt Günther⁴ · Klaus Achterhold^{3,4} · Bernhard Gleich⁴ · Annette Feuchtinger⁵ · Stefan Bartzsch^{1,2} · Elke Beyreuther^{6,7} · Stephanie E. Combs^{1,2,8} · Franz Pfeiffer^{3,4,9} · Jan J. Wilkens^{2,3} · Thomas E. Schmid^{1,2} 

Received: 27 February 2019 / Accepted: 14 October 2019 / Published online: 26 October 2019
© Springer-Verlag GmbH Germany, part of Springer Nature 2019

Abstract

Microbeam radiation therapy (MRT), a preclinical form of spatially fractionated radiotherapy, uses an array of microbeams of hard synchrotron X-ray radiation. Recently, compact synchrotron X-ray sources got more attention as they provide essential prerequisites for the translation of MRT into clinics while overcoming the limited access to synchrotron facilities. At the Munich compact light source (MuCLS), one of these novel compact X-ray facilities, a proof of principle experiment was conducted applying MRT to a xenograft tumor mouse model. First, subcutaneous tumors derived from the established squamous carcinoma cell line FaDu were irradiated at a conventional X-ray tube using broadbeam geometry to determine a suitable dose range for the tumor growth delay. For irradiations at the MuCLS, FaDu tumors were irradiated with broadbeam and microbeam irradiation at integral doses of either 3 Gy or 5 Gy and tumor growth delay was measured. Microbeams had a width of 50 μm and a center-to-center distance of 350 μm with peak doses of either 21 Gy or 35 Gy. A dose rate of up to 5 Gy/min was delivered to the tumor. Both doses and modalities delayed the tumor growth compared to a sham-irradiated tumor. The irradiated area and microbeam pattern were verified by staining of the DNA double-strand break marker γH2AX . This study demonstrates for the first time that MRT can be successfully performed in vivo at compact inverse Compton sources.

Keywords MRT · Microbeam · Inverse Compton X-ray sources · Tumor · X-rays · Growth delay

Introduction

Microbeam radiation therapy (MRT) is a preclinical, spatially fractionated form of radiation therapy (Slatkin et al. 1992, 1995; Laissue et al. 1998). MRT deposits very high doses, also referred to as peak dose, in parallel and

planar beams with a width of 25–75 μm and a spacing of 100–400 μm . Also beams with a width of 680 μm (Dilmanian et al. 2006) or 950 μm (Anschel et al. 2007) were able to spare normal tissue and control tumors. The deposited dose between two microbeams is lower than the tolerance dose of the normal tissue. This so-called valley dose is influenced by

✉ Thomas E. Schmid
thomas.schmid@helmholtz-muenchen.de

¹ Institute of Radiation Medicine, Helmholtz Zentrum München GmbH, 85764 Neuherberg, Germany

² Department of Radiation Oncology, School of Medicine, Klinikum rechts der Isar, Technical University of Munich, 81675 Munich, Germany

³ Chair of Biomedical Physics, Department of Physics, Technical University of Munich, 85748 Garching, Germany

⁴ Munich School of BioEngineering, Technical University of Munich, 85748 Garching, Germany

⁵ Research Unit Analytical Pathology, Helmholtz Zentrum München GmbH, 85764 Neuherberg, Germany

⁶ Helmholtz-Zentrum Dresden-Rossendorf, 01328 Dresden, Germany

⁷ OncoRay, National Center for Radiation Research in Oncology, Faculty of Medicine, University Hospital Carl Gustav Carus, Technische Universität Dresden, Helmholtz-Zentrum Dresden-Rossendorf, 01328 Dresden, Germany

⁸ German Consortium for Translational Cancer Research, Deutsches Konsortium für Translationale Krebsforschung (dtk), Technical University Munich, 81675 Munich, Germany

⁹ Department of Diagnostic and Interventional Radiobiology, School of Medicine, Klinikum rechts der Isar, Technical University of Munich, 81675 Munich, Germany

scattering of secondary electrons and photons from adjacent peaks (Sabatasso et al. 2011).

First in vitro and in vivo experiments focusing on tumoricidal effects of spatially fractionated irradiations were performed at large synchrotron radiation facilities such as the European Synchrotron Radiation Facility in France (Regnard et al. 2008; Bouchet et al. 2010, 2016; Gil et al. 2011; Fardone et al. 2018). Owing to their ultra-high dose rates of hundreds of Gray per second and a small beam divergence, synchrotrons are particularly suited to maintain the microbeam pattern within the tissue without blurring (Bartzsch and Oelfke 2017). Synchrotron-generated X-ray MRT induces a differential radiobiological response in tumor and normal tissues. While the normal tissue is exceptionally tolerant to the high doses in the peak regions, the tumor growth is delayed and even sometimes controlled after MRT (Laissue et al. 1998; Serduc et al. 2009; Bouchet et al. 2010; Crosbie et al. 2010). The mechanisms playing a role in the differential response of tumor and normal tissue are still unknown but there is some evidence of a differential repair of the vasculature as well as bystander effects which are, at least in part, responsible for the sparing effect (Dilmanian et al. 2007).

Patients with tumors in brain or lung surrounded by radiosensitive normal tissues would especially benefit from the pronounced tissue sparing effect of MRT (Ibahim et al. 2014; Archer et al. 2017). However, the use of synchrotrons for cancer treatment with MRT in clinics is hampered by the large space requirements and their cost-intensive operation (Bartzsch and Oelfke 2017). Therefore, in recent years new compact X-ray sources were developed such as the carbon nanotube X-ray source (Hadsell et al. 2013) or the compact light source (CLS) (Eggl et al. 2016). CLSs are based on the concept of inverse Compton scattering. Inverse Compton scattering is a collision between electrons and laser photons producing nearly monochromatic X-rays. The CLS, located in Garching (Germany) and manufactured by Lyncean Technologies Inc., USA, is a compact synchrotron source producing X-rays with photon energies of 15–35 keV (Eggl et al. 2016; Burger et al. 2017). The unique features of the CLS are a small circumference of the electron storage ring of 4.6 m and a short period of the laser undulator defined by the half of the laser wavelength of 0.5 μm , allowing a size of the source of about $2 \times 7 \text{ m}^2$ (Eggl et al. 2016). In recent years CLS was used for pre-clinical imaging and diagnostic of pulmonary emphysema (Schleede et al. 2012b) or breast cancer (Schleede et al. 2012a) but the CLS can also be adopted for MRT due to its synchrotron-like features.

The tumoricidal effectiveness and the sparing effect of MRT at compact X-ray sources seems to be comparable to previous observations made at synchrotrons. Treatment of brain tumors with MRT generated at the carbon nanotube-based X-ray source extended the lifespan of tumor-bearing

animals compared to an untreated control group (Yuan et al. 2015). In contrast to MRT at synchrotrons using peak doses of more than 100 Gy (Fardone et al. 2018), even lower peak doses of 48 Gy or 72 Gy delayed tumor growth at compact X-ray sources (Yuan et al. 2015). At the beamline of the Munich compact light source (MuCLS), in vitro experiments showed an increased survival of normal tissue cells with a lower frequency of chromosomal aberrations following MRT compared to broadbeam irradiation (Burger et al. 2017).

Both compact X-ray sources (Jacquet and Suortti 2015) and synchrotrons (Prezado et al. 2009) produce X-rays with a mean energy in the keV range. Additionally, compact X-ray sources have the advantage of lower operational costs and a laboratory-sized scale. All these features render compact X-ray sources as suitable candidates for a future implementation of MRT into the clinics. To embed MRT in treatment plans of cancer patients, fundamental research of biological mechanisms and dose concepts of MRT is necessary. Especially, studies using animal models at easily accessible compact sources might help to understand MRT in more detail. Here, we show the first in vivo MRT experiment at the MuCLS, a compact synchrotron X-ray source, and evaluate its tumoricidal effect in a mouse model bearing a xenograft of squamous carcinoma cells. This proof of concept study introduces a compact X-ray source at which MRT can be performed now and which can be used for MRT in vivo studies in the future.

Materials and methods

Mouse ear tumor model

All experiments were performed using female, immunocompromised, 8–10 weeks old NMRI nu/nu mice obtained from Charles River Laboratories (Sulzfeld, Germany). Mice were hosted at the experimental sites of the Klinikum rechts der Isar in Munich according to the respective institutional guidelines and the German animal welfare regulations. The animals were kept at 20–24 °C, 45–60% relative humidity, at 12 h light–dark cycle and fed with commercial laboratory animal diet and water ad libitum. All experiments were approved by the regional animal ethics committee (project license 55.2-1-54-2531-62-2016).

Studies were carried out for the undifferentiated human head and neck cancer cell line FaDu maintained at 37 °C, 5% CO₂ in Dulbecco Modified Eagle's Medium with 1000 mg/ml glucose (Sigma-Aldrich Chemie GmbH, Munich, Germany). The media was supplemented with 10% FBS (Roche AG, Grenzach-Wyhlen, Germany), 2 mM L-glutamine, 1 mM sodium pyruvate, 1% Penicillin/Streptomycin (all Sigma-Aldrich Chemie GmbH, Munich, Germany) and

10 mM HEPES (Thermo Fisher Scientific, Germering, Germany).

The mouse ear tumor model was originally established by the group of Suit et al. in 1965 and recently published as suitable model for low energy irradiation by Beyreuther et al. (2017). In order to suppress the immune response, 2–4 days before tumor cell injection nude mice were whole-body irradiated in a specifically designed cage which allows only a two dimensional movement of the mouse. Whole-body irradiation took place with 4 Gy of 200 kVp 15 mA X-rays filtered by aluminum (Xstrahl Limited, Camberley, UK). Then, 1 µl/g body weight of the antibiotic Convenia (Zoetis Schweiz GmbH, Zürich, Switzerland) was subcutaneously injected into the neck. For tumor cell injection, about 100,000 FaDu tumor cells were resuspended with 50 µl Matrigel (Matrigel Basement Membrane Matrix, Corning, New York, USA). Mice were anesthetized intraperitoneally with a mixture of 1 mg/ml medetomidin, 5 mg/ml midazolam and 0.05 mg/ml fentanyl (in-house production, Klinikum rechts der Isar, Munich, Germany). About 5 µl of the ice-cooled tumor cell suspension were injected subcutaneously between the cartilage and skin at the center of the right ear. The anesthesia was antagonized by subcutaneous injection of AFN (composed of 0.5 mg/ml atipamezole, 5 mg/ml flumazenil and 3 mg/ml fentanyl, in-house production, Klinikum rechts der Isar, Munich, Germany). Tumor growth was measured every second day using a digital caliper of 0.01 mm accuracy (DigiMax 29422, Wiha, Buchs, Switzerland). The location of the tumor at the ear allows size measurement in three dimensions. Tumor volume was determined according to the formula $V = \frac{\pi}{6} \times a \times b \times c$. The length a of the tumor was defined as the size of the tumor parallel to the main blood vessels. The width b is perpendicular to the tumor length in the plane of the mouse ear. Measuring the maximum extension out of this plane, the height c was derived. Tumors with a maximum length of 2 mm and a maximum width of 1.8 mm were included into the experiment. There were no limitations regarding tumor height. A second criterion for tumor irradiation was the color of the tumor which changed from white to red once the tumor was vascularized. Only red-colored tumors were included into the experiment.

Irradiations at a conventional X-ray tube

A pilot study was carried out to estimate X-ray doses which induce a growth delay of xenograft FaDu tumors in the ear. This study was performed at the Small Animal Radiation Research Platform (SARRP, Xstrahl Limited, Camberley, UK) using doses of 3 Gy and 6 Gy (Oppelt et al. 2015) applying 70 kVp X-rays filtered by aluminum. Tumor cells were inoculated in 8 mice from which all animals developed a tumor except one mouse. Therefore, two FaDu

tumor-bearing mice were irradiated per dose group and three FaDu tumor-bearing mice served as a control without irradiation. Irradiation took place with a dose rate of 2.4 Gy/min. For irradiations, a round-shaped field size of 4 mm in diameter was used. The distance between target and X-ray source was 350 mm. The tumor was centered in the irradiation field and homogeneously irradiated perpendicular to the plane of the mouse ear. Dose delivery was verified using a radiochromic film (Gafchromic EBT-3, Ashland, USA). Dose values refer to mean doses over the central area of the field as measured with radiochromic film (calibrated with an ionization chamber in an open field) before the actual experiment was performed.

On the day of irradiation, the tumor had to fulfill the pre-defined criteria for size and color. Tumor growth was determined during a follow-up period of about 30 days. Volume measurements were stopped earlier if one tumor dimension reached 8 mm (abort criteria). Growth delay of irradiated tumors was compared to unirradiated control tumors.

Tumor irradiation at MuCLS and follow-up

The radiobiological effect was compared between micro-beam and broadbeam irradiation by determining the radiation-induced tumor growth delay at the MuCLS (CLS from Lyncean Technologies Inc., Fremont, USA) situated at the Munich School of BioEngineering in Garching (Germany). Tumor growth delay was compared between treated animals and one sham-irradiated animal. Tumor cells were inoculated in seven mice in total from which two animals were used as a reserve because the pre-experiment at the SARPP showed a tumor inoculation rate below 100%. For each dose group and modality, one tumor-bearing mouse was irradiated with either sham, microbeams or broadbeams at 3 Gy or 5 Gy at the MuCLS, respectively.

The CLS was operated with a mean energy of 25 keV X-rays having a bandwidth of 3.6%. The distance between the X-ray source and a dedicated irradiation system to treat the mouse ear was 4 m. Besides dose monitoring, the irradiation system comprises means for mouse positioning and maintaining the body temperature. The dose rate and the delivered dose at the plane of the ear was calculated from the measured photon flux. For this purpose, we used an in-house built, highly transmissible intensity counter (online monitor) which was placed into the beam in front of the irradiation target. The intensity counter was calibrated using a photon-counting detector (Pilatus 200 K, Dectris Ltd., Baden, Switzerland). The dose distribution of microbeam pattern (see below) including the peak-to-valley dose ratio (PVDR) was determined using radiochromic film (Gafchromic EBT-3, Ashland, UK) and accompanying Monte Carlo simulations (GEANT4). More details of the technical implementation, characterization, commissioning and dosimetry are reported

in a separate paper (Burger et al. in preparation), basic information about the MuCLS are reported in Eggl et al. (2016).

On the day of irradiation, the tumor had to fulfill the pre-defined criteria for size and color. Animals were anesthetized as described for tumor cell injection (see section mouse ear tumor model). All treated mice were anesthetized for a maximum time of 1 h. This time includes time for positioning of the mouse into the holder, time for positioning of the tumor within the X-ray beam, and time for irradiation. The sham-irradiated mouse was anesthetized for about 30 min and fixed in the mouse holder for 16 min. This time is in the range of the mean time of fixation of irradiated animals. The 3 Gy MRT irradiated mouse was anesthetized for 41 min with a fixation time of 25 min and 5 min for irradiation. The 5 Gy MRT irradiated mouse was anesthetized for 50 min, fixed for 29 min and irradiated for 10 min. The 3 Gy broadbeam irradiated mouse was anesthetized for 32 min, fixed in the mouse holder for 11 min and irradiated for 43 s. The 5 Gy broadbeam irradiated mouse was anesthetized for 27 min, fixed for 10 min and irradiated for 80 s.

The ear of the anesthetized mouse was fixed onto the mouse holder with removable tape (Fig. 1a). Additional heating to 32–33 °C allowed the maintenance of the body temperature of the anesthetized mouse. Tumors were positioned in the middle of the irradiation field and irradiated perpendicular to the plane of the mouse ear. A positioning system allowed for accurate placement of the tumor in the X-ray beam with a circular irradiation field of 2.3 mm in diameter. Tumor-bearing mice were randomly assigned to the following irradiation groups: sham, microbeam or broadbeam irradiation. Tumors were irradiated with an integral dose of either 3 Gy or 5 Gy. These doses for broadbeam irradiations were chosen with the aim to compare the same integrated doses for broadbeam and microbeam irradiations. Therefore, tumors were irradiated with microbeams using peak doses of either 21 Gy or 35 Gy and valley doses below 0.2 Gy, respectively. Microbeams with a width of 50 μm and

a center-to-center distance of 350 μm were generated using a highly absorbing tungsten collimator with a ratio of 1/7 slit to 6/7 tungsten. The irradiation pattern and dose to each irradiated tumor was verified individually by a radiochromic film (Gafchromic EBT-3, Ashland, USA) (Fig. 1b). For this, the radiochromic film was positioned behind the tumor of each mouse. Sham irradiation follows the same protocol with exception that the X-ray beam remained switched off.

Irradiations took place with a dose rate up to 5 Gy/min for broadbeam and 0.6 Gy/min for microbeams. The dose rate was measured as integrated dose rate. Since 6/7 of the broadbeam radiation field were blocked by the tungsten collimator, the integrated dose rate is a factor of 7 lower than in the broadbeam field. On top, scattering led to a slight reduction of the dose rate. The peak dose rate was in the order of 4.2 Gy/min. Hence peak dose rate and broadbeam dose rate are comparable. On average, microbeam irradiation applying an integral dose of either 3 Gy or 5 Gy took about 5.6 ± 0.8 min or 9.5 ± 1.3 min, respectively. For broadbeam irradiation, 0.9 ± 0.3 min and 1.2 ± 0.4 min were necessary for 3 Gy or 5 Gy, respectively.

After irradiation the animals were retained in quarantine during the follow-up period. Tumor growth was measured as described before (see section mouse ear tumor model). Mice were euthanized as soon as one tumor dimension reached 8 mm (Fig. 1c).

Staining of γH2AX on histological tumor sections

To prove the irradiated area and microbeam pattern, tumor cells were inoculated in two additional animals which were irradiated at the MuCLS and assigned to histological analysis. Tumor sections were stained with hematoxylin and eosin (H&E). Staining of the DNA double-strand break marker γH2AX was performed to verify irradiation side and pattern retrospectively. The treated animal was sacrificed 1 h after microbeam irradiation when the maximum expression

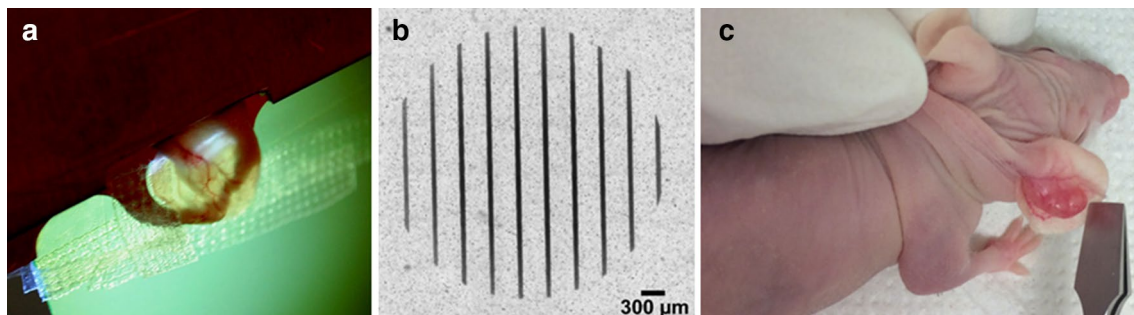


Fig. 1 **a** Tumor-bearing mouse ear is fixed with tapes onto the holder. The FaDu tumor has a size of 2 mm in diameter and is red-colored on day of irradiation. **b** Radiochromic film placed behind the ear was irradiated using microbeams with an integral dose of 5 Gy. Micro-

beam pattern with a beam width of 50 μm and a spacing of 300 μm is visible. **c** Illustration of the tumor size at the end of the follow-up period of tumor growth delay experiment

of γ H2AX is assumed (Kinner et al. 2008). The tumor was resected and fixed in 4% (w/v) neutrally buffered formalin, embedded in paraffin and cut into 3 μ m slices for H&E staining or for immunohistochemistry. Immunohistochemical staining was performed under standardized conditions on a Discovery XT automated stainer (Ventana Medical Systems, Tucson, Arizona) using rabbit anti- γ H2AX (1:500, NB100384, NOVUS Biologicals, Wiesbaden, Germany) as a primary antibody and Discovery Universal (Ventana Medical Systems, Tucson, Arizona) as secondary antibody. Signal detection was conducted using the Discovery[®] DAB Map Kit (Ventana Medical Systems, Tucson, Arizona). The stained tissue sections were scanned with an AxioScan.Z1 digital slide scanner (Zeiss, Jena, Germany) equipped with a 20 \times magnifying objective.

Results

Pilot study for tumor growth delay after broadband irradiation at SARRP

Tumor cells were subcutaneously injected into the ear of NMRI nude mice. Tumors developed and grew to a size of 2 mm in diameter at which homogeneous irradiation took place. Changes in tumor volume were measured after both 3 Gy and 6 Gy at the SARRP. Figure 2 shows the FaDu tumor growth delay over a period of 25 days. In total, two tumors were irradiated with either 3 Gy or 6 Gy of broadband. Three mice served as controls. Control tumors had a volume doubling time of 2.76 ± 0.4 days. At 3 Gy tumor growth was delayed in one of two mice. Following 6 Gy

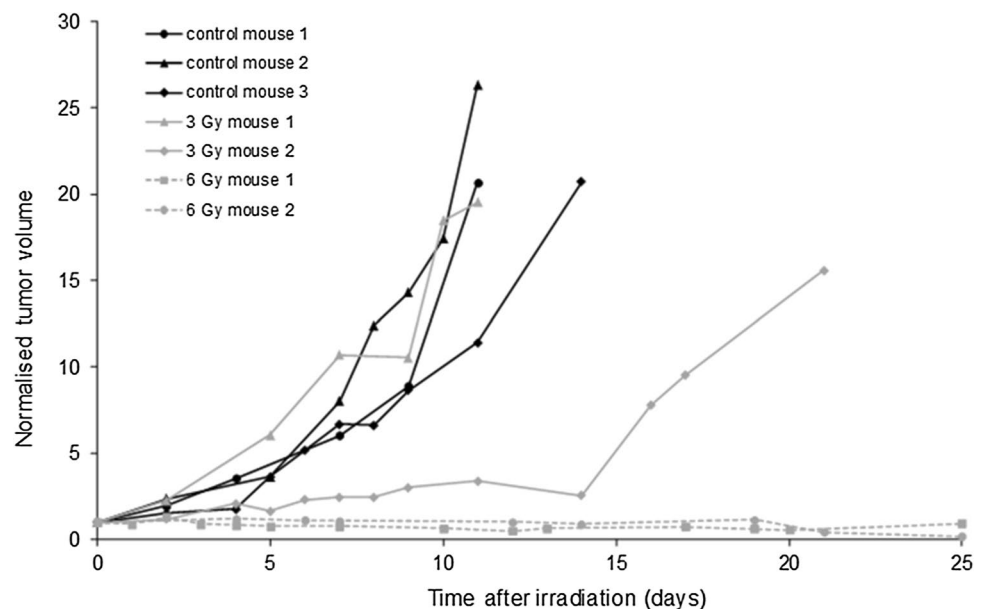
broadbeam irradiation, both FaDu tumors were controlled in their growth.

From this pre-study, we concluded that a dose between 3 Gy and 5 Gy might cause a measurable tumor growth delay at the MuCLS. X-rays of 25 keV at the MuCLS are radiobiological more effective and should therefore be able to induce a clear growth delay at 3 Gy. Furthermore, an integral dose of 5 Gy was chosen in order to have a difference of X-ray doses big enough to resolve a difference between both used doses. A dose higher than 5 Gy was not possible to choose due to the narrow dose range for tumor growth delay as shown in the pre-study. In addition, due to the higher radiobiological effectiveness of 25 keV X-rays a dose higher than 5 Gy could be able to induce a tumor control at the MuCLS which should be avoided. With the aid of the growth delay curves after broadband irradiation, the 15-fold of initial volume was used for calculation of the growth delay of irradiated tumors in comparison to the sham-irradiated tumor at the MuCLS.

Tumor inoculation rate of FaDu tumor cells into mouse ears

FaDu tumor cells were inoculated in eight mice for the pre-experiment at the SARRP. Out of eight, only seven developed a tumor. The tumor inoculation rate is about 87%. For tumor growth delay at the MuCLS, tumor cells were inoculated in seven animals and in two additional animals for histological analysis. Out of nine mice, tumors in seven animals become visible and grew to the particular size on day of irradiation. Four tumor-bearing animals were irradiated with either broadband or microbeam, and one tumor-bearing animal was used as a sham-irradiated

Fig. 2 Growth delay of individual FaDu tumors without irradiation (black lines) and after broadband irradiation with either 3 Gy (grey lines) or 6 Gy (grey dashed lines) using 70 kVp X-rays at the SARRP



control for studying tumor growth delay at the MuCLS. Two tumor-bearing animals were irradiated for histological analysis. In summary, tumors inoculation was successful in around 77% of all animals for irradiation at the MuCLS.

Effect of microbeam irradiation at the MuCLS on tumor growth

Five tumors were irradiated with either sham, microbeams or broadbeam using an integral dose of either 3 Gy or 5 Gy, respectively. After irradiation, tumor growth was recorded until the tumors reached at least their 15-fold initial volume, as determined in the previous pilot study.

Figure 3 shows the tumor volume normalized to the volume on the day of irradiation over time for one mouse per treatment group. The tumor growth curves were linearly interpolated. This preliminary data indicates that growth of all irradiated tumors was delayed compared to the sham-irradiated tumor. The time reaching the 15-fold initial volume increased with increasing integrated dose from 3 Gy to 5 Gy, independently from the radiation modality. On day 21 after irradiation, the sham-irradiated tumor reached the 15-fold volume. After 3 Gy MRT and 5 Gy MRT, tumor growth was delayed and the 15-fold initial volume was reached 3.5 days and 13.5 days later, respectively, compared to the sham-irradiated tumor. For broadbeam irradiations, the 15-fold initial volume was estimated at day 30 and day 37.5 after 3 Gy and 5 Gy, respectively. This corresponds to a tumor growth delay of 9 days for 3 Gy broadbeam irradiated tumors and for 16.5 days for 5 Gy broadbeam irradiated tumors compared to sham-irradiated tumors. To conclude, these preliminary

data show that MRT can induce a tumor growth delay and MRT studies can be performed at the MuCLS now.

γ H2AX staining of a tumor after microbeam irradiation at MuCLS

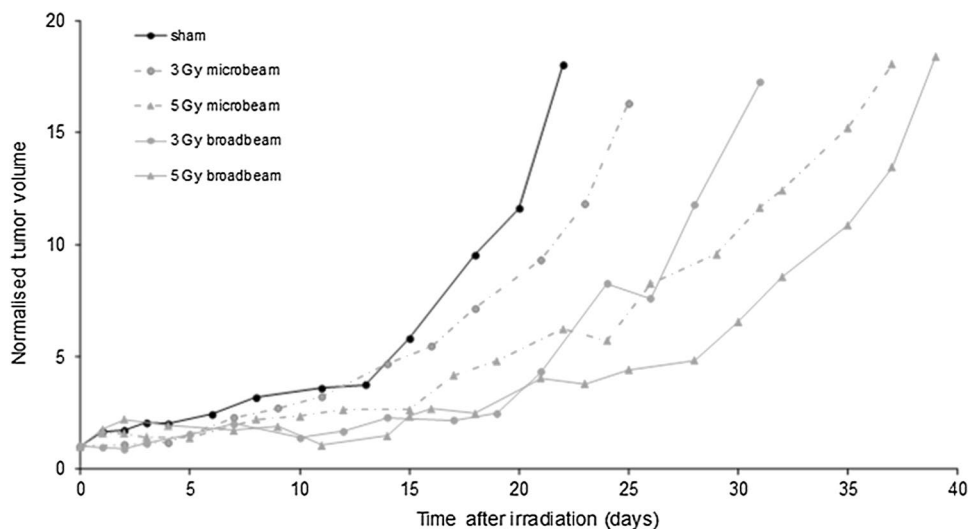
Figure 4a illustrates the FaDu xenograft tumor of one out of two animals on day of irradiation. Tumor cells were grown in nodules surrounded by matrigel, clearly separated from the surrounding tissue and above the cartilage. Figure 4b, c show exemplarily the microbeam pattern, observed 1 h after microbeam irradiation of 5 Gy. The whole area of the injection side of tumor cells mixed with matrigel was irradiated with a total of eight microbeams. The lines with γ H2AX stained cells clearly correlate with the used microbeam width of 50 μ m. In addition, the center-to-center distance of microbeams on the immunologically stained ear sections matches with the pattern given by the tungsten collimator (beam width of 350 μ m).

Discussion

This in vivo study demonstrates that microbeam irradiation can be performed at the MuCLS using a compact synchrotron X-ray source. Microbeam and broadbeam irradiations at the MuCLS were able to induce a tumor growth delay in one mouse, respectively, compared to one sham-irradiated tumor using X-rays with a mean energy of 25 keV. The irradiation pattern of microbeams was confirmed by staining of γ H2AX.

The comparison of the tumoricidal effect between microbeam and broadbeam irradiation at the MuCLS can be done only with caution. In our proof of concept study, we used only one tumor-bearing mouse per treatment group which is

Fig. 3 Normalized tumor volumes over the follow-up period after sham irradiation (black line), microbeam irradiation (grey dashed lines) and broadbeam irradiation (grey lines) using 25 keV X-rays at the MuCLS. One mouse per treatment was monitored until the tumor reached the 15-fold initial volume



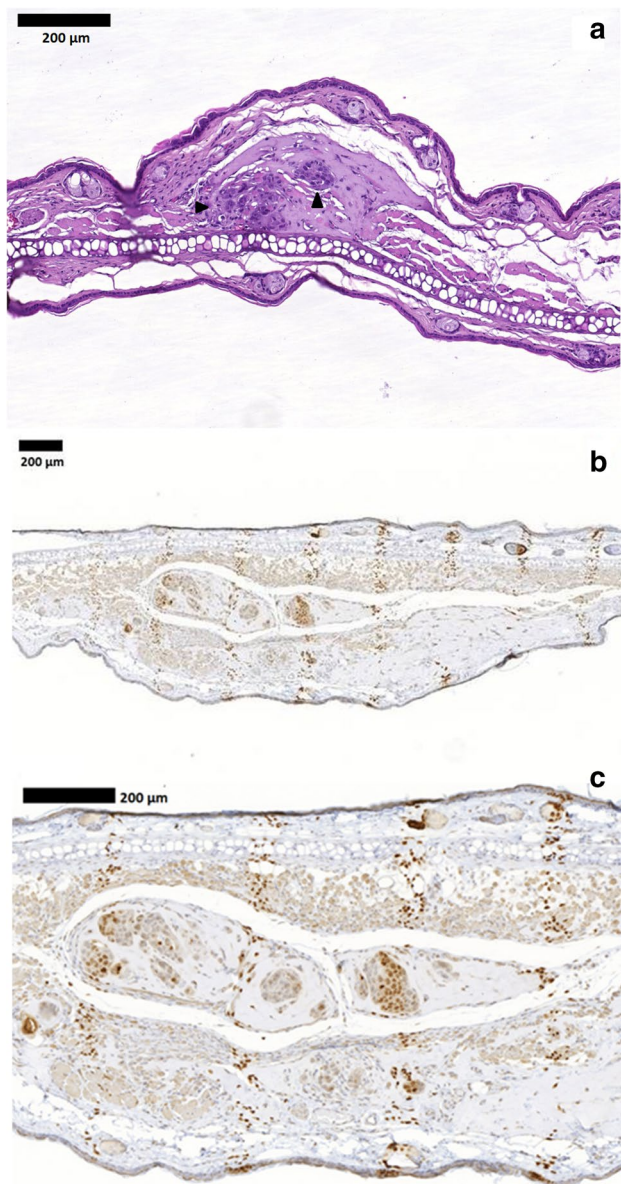


Fig. 4 Histological analysis of FaDu tumors in mouse ears after 5 Gy microbeam irradiation at the MuCLS. Ear sections were stained with **a** hematoxylin and eosin ($\times 10$ magnification) or **b**, **c** γ H2AX 1 h post-irradiation. Image **b** has a $\times 5$ magnification. In **a** the tumor is marked by arrow heads. In **c** the same tumor as depicted in **b** is shown with a higher magnification of $\times 10$ to illustrate the microbeam width of 50 μ m and a separation of 300 μ m. Only the part of the ear harboring the tumor is shown

not statistically representative and therefore does not allow a solid conclusion on the tumoricidal effect of MRT at the MuCLS. Nevertheless, our preliminary results give a hint that the delay of tumor growth is increased after broadbeam irradiations compared to microbeam irradiations if integral doses of 3 Gy and 5 Gy were compared. This observation is contradicted to the well-studied advantageous effect of MRT

(Dilmanian et al. 2002; Regnard et al. 2008). From a technical point of view, a possible explanation for the reduced inhibitory effect of microbeam irradiations on tumor growth could be the delivered peak and valley dose at the MuCLS. Most of the *in vivo* studies used much higher doses in the valley and peak region of around 20 Gy and several hundred Gy, respectively (Dilmanian et al. 2002; Serduc et al. 2009). At the MuCLS, FaDu tumors were irradiated with very low peak doses of either 21 Gy or 35 Gy and a quite constant valley dose below 0.2 Gy. A second important, technical parameter for tumor growth inhibition is the PVDR. The PVDR should be low in the tumor to inhibit any repair mechanisms (Prezado et al. 2009) and thus decrease the rate of tumor growth. In the MRT study of Serduc et al. (2009) PVDRs were used between 18 and 48. This is in contrast to our study at the MuCLS applying much higher PVDRs meaning a lower valley dose which might contribute to an increased DNA damage repair and therefore contribute to an increased tumor growth after microbeam irradiation. A third technical parameter influencing tumor growth inhibition could be the dose rate which was much lower (0.6 Gy/min) at the MuCLS compared to MRT studies at synchrotrons using more than 100 Gy/s (Chtcheprov et al. 2014). However, it has been shown that ultra-high dose rates (≥ 40 Gy/s, FLASH) can be as efficient as conventional dose rates (≤ 0.03 Gy/s) in suppression of tumor growth (Favaudon et al. 2014). Animal studies using ultra-high dose rates for MRT at synchrotrons showed a pronounced tumor growth inhibition. However, according to Favaudon et al. (2014) the low dose rate used at the MuCLS should not be the reason for the observed weak tumor growth delay after microbeam irradiation since the dose rate of 0.6 Gy/min for microbeam irradiation corresponds to 0.01 Gy/s, which is in the range of the conventional dose rates as suggested by Favaudon et al. (2014). From a biological point of view, the reduced inhibitory effect of MRT on tumor growth is in agreement with another MRT study at a compact X-ray source. It has been shown that low peak doses of 48 Gy in combination with low valley doses below 5 Gy only slightly decrease tumor growth after microbeam irradiation compared to broadbeam irradiation (Zhang et al. 2014; Yuan et al. 2015). This less pronounced tumor growth inhibition after microbeam irradiations shown in both studies at compact X-rays sources might be attributed to the absence of a direct cytotoxic effect due to a too low valley dose below 0.2 Gy at the MuCLS inducing subsequently no or only a reduced necrosis in the entire tumor. A similar conclusion was drawn in a 9L brain tumor model using even a much higher valley dose of 24 Gy (Serduc et al. 2008). In addition to that, MRT-induced tumor vascular damage can also affect tumor growth. It has been shown that peak doses of 75 Gy and 150 Gy are able to decrease the vascular density and reduce oxygenation resulting in a prominent tumor growth delay (Griffin et al. 2012). The damage of the tumor

vasculature can be long-lasting after applying an entrance dose of more than 100 Gy to tumors (Griffin et al. 2012; Bouchet et al. 2015). However, a dose of 20 Gy, which is in the range of the applied peak doses at the MuCLS, is able to induce only a transient damage of the vasculature of a xenograft tumor which subsequently recovers after some days (Kim et al. 2013). This indicates that a peak dose of 21 Gy or 35 Gy at the MuCLS could be too low for persistent damage of the tumor vasculature and thereby result in a reduced tumor growth inhibition. However, a solid conclusion of a tumor growth inhibition of microbeam irradiation at the MuCLS at 3 Gy and 5 Gy can only be drawn, if more animals will be irradiated with microbeams and broadbeams.

Furthermore, our MRT study gives a hint that there is an increased tumor growth inhibition after applying a high integral dose of 5 Gy compared to an integral dose of 3 Gy. It was measured for both treatment modalities. Although this observation cannot be proven statistically due to the low number of animals per treatment group, it is in line with the study of Dilmanian et al. (2002) demonstrating a higher tumor control after delivering of higher peak doses and using a constant valley dose.

In our study, tumors were irradiated with 50 μm wide microbeams which were separated by 350 μm . The paths of microbeams can be detected by staining of γH2AX which is known as DNA double-strand break marker (Fernandez-Palomo et al. 2015). The width and the spacing between two adjacent microbeams agree to the γH2AX positively stained paths on ear sections. The immunohistochemical staining of γH2AX also shows that there is no blurring of microbeams present. Blurring of microbeams, which results in broader beam widths and lower peak-to-valley dose ratios, can happen due to respiration-induced tumor motion (Chtcheprov et al. 2014). Motion effects are more likely observed when abdominal tumors (e.g. in liver or brain) are irradiated (Serduc et al. 2010; Chtcheprov et al. 2014). At synchrotrons, motion blur can be reduced due to ultra-high dose rates of more than 100 Gy/s (Chtcheprov et al. 2014). Treating different targets, motion during microbeam irradiation at low dose rates might play an important role, which has not yet been investigated.

A technical limitation of our study was the small circular irradiation field of 2.3 mm in diameter which corresponds to the maximum tumor size plus a safety margin to irradiate. This tumor size is small compared to tumor sizes which are conventionally irradiated in tumor growth delay assays in the hind limb. Subcutaneous tumors in the hind limb have typically a size of about $8 \times 4 \text{ mm}^2$ on day of irradiation (Zlobinskaya et al. 2014). The recently developed mouse model for growth delay studies of small subcutaneous tumors is the mouse ear tumor model where tumor cells were injected subcutaneously in the ear. This mouse ear tumor model allows the irradiation of tumors with a minimum size

of 2 mm (Oppelt et al. 2015). Moreover, mouse ears have the advantage of a small thickness of about 215–250 μm (Girst et al. 2016; Dombrowsky et al. 2019) which allows penetration of low energy X-rays and thus, the treatment of shallow-seated tumors. In previous studies, the mouse ear tumor model showed a stable and high tumor take rate (Beyreuther et al. 2017). A tumor take rate of around 100% has been recorded after inoculation of FaDu cells combined with pure matrigel (Beyreuther et al. 2017). In our pilot-study, we observed a quiet high tumor take rate of 87.5%. However, it was reduced to 77% in the growth delay study at the MuCLS. This difference could be explained by failure in handling such as a lower injected cell concentration or inadequate mixture of cell suspension before injection. A well-known drawback of the FaDu tumor mouse ear model is a high risk of secondary tumors (Beyreuther et al. 2017). In our study, secondary tumors developed at neck or base of the right ear in 20% of all inoculated mice.

It has been shown that tumor growth can be delayed within a dose range of 3.8 Gy to 7.9 Gy after 200 kV X-rays (Beyreuther et al. 2017). In line with these results, our study at the MuCLS demonstrates that doses of 3 Gy and 5 Gy of broadbeam irradiations seems to be able to delay tumor growth at the considerably lower X-ray energy of 25 keV. However, a reliable conclusion can only be drawn as soon as more animals will be irradiated. The single sham-irradiated tumor at the MuCLS reached the 15-fold initial volume on day 21 after irradiation. In contrast to that, at the SARRP control tumors reached the abort criterion on day 12 for the latest. The slower tumor growth in the MuCLS study might be ascribed to a stressful handling due to transportation from the animal house to the radiation facility and vice versa. Another reason for a disturbed tumor growth could be the animal housing under quarantine conditions after irradiation at the MuCLS.

The low dose rate of compact X-ray sources is often discussed as a restriction of performing MRT in mouse models (Yuan et al. 2015; Bartzsch and Oelfke 2017). The CLS can be operated with a dose rate of 0.6 Gy/min for MRT which is in a comparable range of other novel compact microbeam sources, such as the carbon nanotube-based irradiator with a dose rate of 1.2 Gy/min (Yuan et al. 2015). Due to recently installed system upgrades at the MuCLS, higher dose rates are expected for future experiments. Nevertheless, the feasible dose rates of compact X-ray sources are much lower than the ultra-high dose rates of hundreds of Gray per second typically used in MRT studies at synchrotron facilities (Fardone et al. 2018). Despite the much lower dose rate at the MuCLS, our study gives a hint that the tumor volume growth could be reduced after microbeam irradiation at both 3 Gy and 5 Gy. Most previous experiments on the dose rate showed that dose rate effects become relevant for dose rates below 1 Gy/min (Joiner and Van der Kogel 2009) and

exposure time above around 10 min. For this reason, dose rate effects play a negligible role in our experiment at the MuCLS. For future studies, further technical improvements which are partially already implemented should achieve an increase in size of the irradiation field, higher dose rates and peak doses for comparable MRT studies at compact X-ray sources and synchrotron facilities.

In conclusion, this proof of principle experiment introduces a novel compact X-ray source for preclinical MRT studies. The tumoricidal effect of MRT, even at low peak and valley doses, delivered by the CLS can be expected but needs to be proven with a higher number of animals. These findings deliver important insights into the necessary dose delivery of microbeam irradiations at compact microbeam sources.

Acknowledgements This work has been supported by the Deutsche Forschungsgemeinschaft (MAP C.3.4, CALA) Cluster of Excellence: Munich-Centre for Advanced Photonics as well as the Munich School of BioEngineering of the Technical University of Munich. This work was also supported by the Centre of Advanced Laser Applications with respect to resources necessary for and at the Munich Compact Light Source.

Compliance with ethical standards

Conflict of interest The authors declare they have no actual or potential competing financial interests.

Ethical approval All applicable national and institutional guidelines for the care and use of animals were followed. All procedures performed in this study involving animals were in accordance with ethical standards of the institution at which the study was conducted (project license 55.2-1-54-2531-62-2016).

References

- Anschel DJ, Romanelli P, Benveniste H, Foerster B, Kalef-Ezra J, Zhong Z, Dilmanian FA (2007) Evolution of a focal brain lesion produced by interlaced microplanar X-rays. *Minim Invasive Neurosurg* 50:43–46. <https://doi.org/10.1055/s-2007-976514>
- Archer J, Li E, Petasecca M, Dipuglia A, Cameron M, Stevenson A, Hall C, Hausermann D, Rosenfeld A, Lerch M (2017) X-ray microbeam measurements with a high resolution scintillator fibre-optic dosimeter. *Sci Rep* 7:12450. <https://doi.org/10.1038/s41598-017-12697-6>
- Bartzsch S, Oelfke U (2017) Line focus X-ray tubes—a new concept to produce high brilliance X-rays. *Phys Med Biol* 62:8600–8615. <https://doi.org/10.1088/1361-6560/aa910b>
- Beyreuther E, Bruchner K, Krause M, Schmidt M, Szabo R, Pawelke J (2017) An optimized small animal tumour model for experimentation with low energy protons. *PLoS One* 12:e0177428. <https://doi.org/10.1371/journal.pone.0177428>
- Bouchet A, Lemasson B, Le Duc G, Maisin C, Bräuer-Krisch E, Siegbahn EA, Renaud L, Khalil E, Rémy C, Poillot C, Bravin A, Laissue JA, Barbier EL, Serduc R (2010) Preferential effect of synchrotron microbeam radiation therapy on intracerebral 9L gliosarcoma vascular networks international. *J Radiat Oncol Biol Phys* 78:1503–1512. <https://doi.org/10.1016/j.ijrobp.2010.06.021>

- Bouchet A, Serduc R, Laissue JA, Djonov V (2015) Effects of microbeam radiation therapy on normal and tumoral blood vessels. *Phys Med* 31:634–641. <https://doi.org/10.1016/j.ejmp.2015.04.014>
- Bouchet A, Brauer-Krisch E, Prezado Y, El Atifi M, Rogalev L, Le Clec'h C, Laissue JA, Pelletier L, Le Duc G (2016) Better efficacy of synchrotron spatially microfractionated radiation therapy than uniform radiation therapy on glioma. *Int J Radiat Oncol Biol Phys* 95:1485–1494. <https://doi.org/10.1016/j.ijrobp.2016.03.040>
- Burger K, Ilicic K, Dierolf M, Gunther B, Walsh DWM, Schmid E, Ettl E, Achterhold K, Gleich B, Combs SE, Molls M, Schmid TE, Pfeiffer F, Wilkens JJ (2017) Increased cell survival and cytogenetic integrity by spatial dose redistribution at a compact synchrotron X-ray source. *PLoS One* 12:e0186005. <https://doi.org/10.1371/journal.pone.0186005>
- Chitchevov P, Burk L, Yuan H, Inscoc C, Ger R, Hadsell M, Lu J, Zhang L, Chang S, Zhou O (2014) Physiologically gated microbeam radiation using a field emission X-ray source array. *Med Phys* 41:081705. <https://doi.org/10.1118/1.4886015>
- Crosbie JC, Anderson RL, Rothkamm K, Restall CM, Cann L, Ruwamura S, Meachem S, Yagi N, Svalbe I, Lewis RA, Williams BRG, Rogers PAW (2010) Tumor cell response to synchrotron microbeam radiation therapy differs markedly from cells in normal tissues. *Int J Radiat Oncol Biol Phys* 77:886–894. <https://doi.org/10.1016/j.ijrobp.2010.01.035>
- Dilmanian FA, Button TM, Le Duc G, Zhong N, Pena LA, Smith JA, Martinez SR, Bacarian T, Tammam J, Ren B, Farmer PM, Kalef-Ezra J, Micca PL, Nawrocky MM, Niederer JA, Recksiek FP, Fuchs A, Rosen EM (2002) Response of rat intracranial 9L gliosarcoma to microbeam radiation therapy. *Neurooncology* 4:26–38
- Dilmanian FA, Zhong Z, Bacarian T, Benveniste H, Romanelli P, Wang R, Welwart J, Yuasa T, Rosen EM, Ansel DJ (2006) Interlaced X-ray microplanar beams: a radiosurgery approach with clinical potential. *Proc Natl Acad Sci USA*. <https://doi.org/10.1073/pnas.0603567103>
- Dilmanian FA, Qu Y, Feinendegen LE, Pena LA, Bacarian T, Henn FA, Kalef-Ezra J, Liu S, Zhong Z, McDonald JW (2007) Tissue-sparing effect of X-ray microplanar beams particularly in the CNS: is a bystander effect involved? *Exp Hematol* 35:69–77. <https://doi.org/10.1016/j.exphem.2007.01.014>
- Dombrowsky AC, Schauer J, Sammer M, Blutke A, Walsh DWM, Schwarz B, Bartzsch S, Feuchtinger A, Reindl J, Combs SE, Dollinger G, Schmid TE (2019) acute skin damage and late radiation-induced fibrosis and inflammation in murine ears after high-dose irradiation. *Cancers*. <https://doi.org/10.3390/cancers11050727>
- Ettl E, Dierolf M, Achterhold K, Jud C, Gunther B, Braig E, Gleich B, Pfeiffer F (2016) The Munich compact light source: initial performance measures. *J Synchrotron Radiat* 23:1137–1142. <https://doi.org/10.1107/s160057751600967x>
- Fardone E, Pouyatos B, Bräuer-Krisch E, Bartzsch S, Mathieu H, Requardt H, Bucci D, Barbone G, Coan P, Battaglia G, Le Duc G, Bravin A, Romanelli P (2018) Synchrotron-generated microbeams induce hippocampal transections in rats. *Sci Rep* 8:184. <https://doi.org/10.1038/s41598-017-18000-x>
- Favaudon V, Caplier L, Monceau V, Pouzoulet F, Sayarath M, Fouillade C, Poupon MF, Brito I, Hupe P, Bourhis J, Hall J, Fontaine JJ, Vozenin MC (2014) Ultrahigh dose-rate FLASH irradiation increases the differential response between normal and tumor tissue in mice. *Sci Transl Med* 6:245–293. <https://doi.org/10.1126/scitranslmed.3008973>
- Fernandez-Palomo C, Mothersill C, Bräuer-Krisch E, Laissue J, Seymour C, Schültke E (2015) γ -H2AX as a marker for dose deposition in the brain of Wistar rats after synchrotron microbeam radiation. *PLoS One* 10:e0119924. <https://doi.org/10.1371/journal.pone.0119924>
- Gil S, Sarun S, Biete A, Prezado Y, Sabés M (2011) Survival Analysis of F98 glioma rat cells following minibeam or broad-beam

- synchrotron radiation therapy. *Radiat Oncol* 6:1–9. <https://doi.org/10.1186/1748-717x-6-37>
- Girst S, Greubel C, Reindl J, Siebenwirth C, Zlobinskaya O, Walsh DW, Ilicic K, Aichler M, Walch A, Wilkens JJ, Multhoff G, Dollinger G, Schmid TE (2016) Proton minibeam radiation therapy reduces side effects in an in vivo mouse ear model. *Int J Radiat Oncol Biol Phys* 95:234–241. <https://doi.org/10.1016/j.ijrobp.2015.10.020>
- Griffin RJ, Koonce NA, Dings RP, Siegel E, Moros EG, Brauer-Krisch E, Corry PM (2012) Microbeam radiation therapy alters vascular architecture and tumor oxygenation and is enhanced by a galectin-1 targeted anti-angiogenic peptide. *Radiat Res* 177:804–812
- Hadsell M, Zhang J, Laganis P, Sprenger F, Shan J, Zhang L, Burk L, Yuan H, Chang S, Lu J, Zhou O (2013) A first generation compact microbeam radiation therapy system based on carbon nanotube X-ray technology. *Appl Phys Lett* 103:183505. <https://doi.org/10.1063/1.4826587>
- Ibrahim MJ, Crosbie JC, Yang Y, Zaitseva M, Stevenson AW, Rogers PA, Paiva P (2014) An evaluation of dose equivalence between synchrotron microbeam radiation therapy and conventional broad beam radiation using clonogenic and cell impedance assays. *PLoS One* 9:e100547. <https://doi.org/10.1371/journal.pone.0100547>
- Jacquet M, Suortti P (2015) Radiation therapy at compact compact sources. *Phys Med* 31:596–600. <https://doi.org/10.1016/j.ejmp.2015.02.010>
- Joiner M, Van der Kogel A (2009) Basic clinical radiobiology, 4th edn. Hodder Education, London
- Kim JW, Lee DW, Choi WH, Jeon YR, Kim SH, Cho H, Lee EJ, Hong ZY, Lee WJ, Cho J (2013) Development of a porcine skin injury model and characterization of the dose-dependent response to high-dose radiation. *J Radiat Res* 54:823–831. <https://doi.org/10.1093/jrr/rrt016>
- Kinner A, Wu W, Staudt C, Iliakis G (2008) Gamma-H2AX in recognition and signaling of DNA double-strand breaks in the context of chromatin. *Nucleic Acids Res* 36:5678–5694. <https://doi.org/10.1093/nar/gkn550>
- Laissue JA, Geiser G, Spanne PO, Dilmanian FA, Gebbers JO, Geiser M, Wu XY, Makar MS, Micca PL, Nawrocky MM, Joel DD, Slatkin DN (1998) Neuropathology of ablation of rat gliosarcomas and contiguous brain tissues using a microplanar beam of synchrotron-wiggler-generated X-rays. *Int J Cancer* 78:654–660. [https://doi.org/10.1002/\(sici\)1097-0215\(19981123\)78:5%3c654::aid-ijc21%3e3.0.co;2-l](https://doi.org/10.1002/(sici)1097-0215(19981123)78:5%3c654::aid-ijc21%3e3.0.co;2-l)
- Oppelt M, Baumann M, Bergmann R, Beyreuther E, Brüchner K, Hartmann J, Karsch L, Krause M, Laschinsky L, Leßmann E, Nicolai M, Reuter M, Richter C, Sävert A, Schnell M, Schürer M, Woithe J, Kaluza M, Pawelke J (2015) Comparison study of in vivo dose response to laser-driven versus conventional electron beam. *Radiat Environ Biophys* 54:155–166. <https://doi.org/10.1007/s00411-014-0582-1>
- Prezado Y, Fois G, Le Duc G, Bravin A (2009) Gadolinium dose enhancement studies in microbeam radiation therapy. *Med Phys* 36:3568–3574. <https://doi.org/10.1118/1.3166186>
- Regnard P, Le Duc G, Brauer-Krisch E, Tropes I, Siegbahn EA, Kusak A, Clair C, Bernard H, Dallery D, Laissue JA, Bravin A (2008) Irradiation of intracerebral 9L gliosarcoma by a single array of microplanar X-ray beams from a synchrotron: balance between curing and sparing. *Phys Med Biol* 53:861–878. <https://doi.org/10.1088/0031-9155/53/4/003>
- Sabatasso S, Laissue JA, Hlushchuk R, Graber W, Bravin A, Brauer-Krisch E, Corde S, Blattmann H, Gruber G, Djonov V (2011) Microbeam radiation-induced tissue damage depends on the stage of vascular maturation. *Int J Radiat Oncol Biol Phys* 80:1522–1532. <https://doi.org/10.1016/j.ijrobp.2011.03.018>
- Schleede S, Bech M, Achterhold K, Potdevin G, Gifford M, Loewen R, Limborg C, Ruth R, Pfeiffer F (2012a) Multimodal hard X-ray imaging of a mammography phantom at a compact synchrotron light source. *J Synchrotron Radiat* 19:525–529. <https://doi.org/10.1107/s0909049512017682>
- Schleede S, Meinel FG, Bech M, Herzen J, Achterhold K, Potdevin G, Malecki A, Adam-Neumair S, Thieme SF, Bamberg F, Nikolaou K, Bohla A, Yildirim AO, Loewen R, Gifford M, Ruth R, Eickelberg O, Reiser M, Pfeiffer F (2012b) Emphysema diagnosis using X-ray dark-field imaging at a laser-driven compact synchrotron light source. *Proc Natl Acad Sci USA* 109:17880–17885. <https://doi.org/10.1073/pnas.1206684109>
- Serduc R, Christen T, Laissue J, Fariou R, Bouchet A, Sanden B, Segebarth C, Brauer-Krisch E, Le Duc G, Bravin A, Remy C, Barbier EL (2008) Brain tumor vessel response to synchrotron microbeam radiation therapy: a short-term in vivo study. *Phys Med Biol* 53:3609–3622. <https://doi.org/10.1088/0031-9155/53/13/015>
- Serduc R, Bouchet A, Brauer-Krisch E, Laissue JA, Spiga J, Sarun S, Bravin A, Fonta C, Renaud L, Boutonnat J, Siegbahn EA, Esteve F, Le Duc G (2009) Synchrotron microbeam radiation therapy for rat brain tumor palliation-influence of the microbeam width at constant valley dose. *Phys Med Biol* 54:6711–6724. <https://doi.org/10.1088/0031-9155/54/21/017>
- Serduc R, Brauer-Krisch E, Siegbahn EA, Bouchet A, Pouyatos B, Carron R, Pannetier N, Renaud L, Berruyer G, Nemoz C, Brochard T, Remy C, Barbier EL, Bravin A, Le Duc G, Depaulis A, Esteve F, Laissue JA (2010) High-precision radiosurgical dose delivery by interlaced microbeam arrays of high-flux low-energy synchrotron X-rays. *PLoS One* 5:e9028. <https://doi.org/10.1371/journal.pone.0009028>
- Slatkin DN, Spanne P, Dilmanian FA, Sandborg M (1992) Microbeam radiation therapy. *Med Phys* 19:1395–1400. <https://doi.org/10.1118/1.596771>
- Slatkin DN, Spanne P, Dilmanian FA, Gebbers JO, Laissue JA (1995) Subacute neuropathological effects of microplanar beams of X-rays from a synchrotron wiggler. *Proc Natl Acad Sci* 92:8783–8787
- Yuan H, Zhang L, Frank JE, Inscoe CR, Burk LM, Hadsell M, Lee YZ, Lu J, Chang S, Zhou O (2015) Treating brain tumor with microbeam radiation generated by a compact carbon-nanotube-based irradiator: initial radiation efficacy study. *Radiat Res* 184:322–333. <https://doi.org/10.1667/rr13919.1>
- Zhang L, Yuan H, Inscoe C, Chtcheprov P, Hadsell M, Lee Y, Lu J, Chang S, Zhou O (2014) Nanotube X-ray for cancer therapy: a compact microbeam radiation therapy system for brain tumor treatment. *Expert Rev Anticancer Ther* 14:1411–1418. <https://doi.org/10.1586/14737140.2014.978293>
- Zlobinskaya O, Siebenwirth C, Greubel C, Hable V, Hertenberger R, Humble N, Reinhardt S, Michalski D, Roper B, Multhoff G, Dollinger G, Wilkens JJ, Schmid TE (2014) The effects of ultra-high dose rate proton irradiation on growth delay in the treatment of human tumor xenografts in nude mice. *Radiat Res* 181:177–183. <https://doi.org/10.1667/rr13464.1>

Publisher's Note Springer Nature remains neutral with regard to jurisdictional claims in published maps and institutional affiliations.